Cerebral Cortex December 2013;23:2803–2817
doi:10.1093/cercor/bhs254
Advance Access publication September 3, 2012

Morphology and Physiology of Excitatory Neurons in Layer 6b of the Somatosensory Rat Barrel Cortex

Manuel Marx[1] and Dirk Feldmeyer[1,2,3]

[1]Research Center Jülich, Institute of Neuroscience and Medicine (INM-2), D-52425 Jülich, Germany, [2]Department of Psychiatry, Psychotherapy and Psychosomatics, Medical School, RWTH Aachen University, D-52074 Aachen, Germany and [3]Jülich Aachen Research Alliance, Translational Brain Medicine (JARA Brain), D-52074 Aachen, Germany

Address correspondence to Dirk Feldmeyer, Research Center Jülich, Institute of Neuroscience and Medicine, INM-2, D-52425 Jülich, Germany. Email: d.feldmeyer@fz-juelich.de

Neocortical lamina 6B (L6B) is a largely unexplored layer with a very heterogeneous cellular composition. To date, only little is known about L6B neurons on a systematic and quantitative basis. We investigated the morphological and electrophysiological properties of excitatory L6B neurons in the rat somatosensory barrel cortex using whole-cell patch-clamp recordings and simultaneous biocytin fillings. Subsequent histological processing and computer-assisted 3D reconstructions provided the basis for a classification of excitatory L6B neurons according to their structural and functional characteristics. Three distinct clusters of excitatory L6B neurons were identified: (C1) pyramidal neurons with an apical dendrite pointing towards the pial surface, (C2) neurons with a prominent, "apical"-like dendrite not oriented towards the pia, and (C3) multipolar spiny neurons without any preferential dendritic orientation. The second group could be further subdivided into three categories termed inverted, "tangentially" oriented and "horizontally" oriented neurons. Furthermore, based on the axonal domain two subcategories of L6B pyramidal cells were identified that had either a more barrel-column confined or an extended axonal field. The classification of excitatory L6B neurons provided here may serve as a basis for future studies on the structure, function, and synaptic connectivity of L6B neurons.

Keywords: axonal domain, cluster analysis, dendritic domain, density maps, neuronal characterization

Introduction

Layer 6 is developmentally the earliest and innermost layer of the distinct six-layered neocortex. During neurogenesis, layer 6 develops at the same time as the subplate (SP; König et al. 1975, 1977; Luskin and Shatz 1985; Valverde et al. 1989; Allendoerfer and Shatz 1994; Ohana and Sakmann 1998). It is commonly divided by a light plexus of fibers into two distinct sublaminae, that is, a broader sublamina (6A) and a narrow sublamina (6B) that borders on the white matter (Marin-Padilla 1978; Tömböl 1984; Ferrer et al. 1986a, 1986b; Valverde et al. 1989; Woo et al. 1991; Zhang and Deschenes 1997). Lamina 6B (L6B) is already distinguishable before birth (Valverde et al. 1989). At present, the function of layer 6B remains somewhat enigmatic and was controversially discussed in the last decades of research. It has been given various names including lamina fusiformis (Vogt and Vogt 1919), layer 6B, deep layer 6(B), or layer 7 (von Economo and Koskina 1925; König et al. 1977; Marin-Padilla 1978; Reep and Goodwin 1988; Woo et al. 1991; McDonald and Burkhalter 1993; DeDiego et al. 1994; Clancy and Cauller 1999), lamina multiformis/infima (Rose 1931; Garweg 1970), deep cortical band (Kristt 1979b), and border layer (Hogan and Berman 1992) although these definitions are not exactly interchangeable. A fraction of L6B neurons is believed to be a remnant cell population from the developmental SP that persists into adulthood (Kostovic and Rakic 1980; Reep and Goodwin 1988; Chun and Shatz 1989; Bayer and Altman 1990; Woo et al. 1991; Clancy and Cauller 1999; Hanganu et al. 2002; for reviews see Torres-Reveron and Friedlander 2007; Friedlander and Torres-Reveron 2009; Kanold and Luhmann 2010). Layer 6B has been analyzed in different neocortical areas of several species with respect to its morphological heterogeneity (Kirsche et al. 1973; Tömböl et al. 1975; Feldman and Peters 1978; Ferrer et al. 1986a, 1986b; Miller and Potempa 1990; Zhang and Deschenes 1997; Clancy and Cauller 1999; Kumar and Ohana 2008; Andjelic et al. 2009; Chen et al. 2009). Only few quantitative studies on the structural and functional properties of L6B neurons are currently available. In addition, the role of Layer 6B in processing sensory information and its contribution to the intracortical neuronal network is largely neglected. Here, we investigate the morphological and some electrophysiological properties of L6B neurons using whole-cell voltage-clamp recordings and simultaneous biocytin fillings to characterize neocortical layer 6B quantitatively. We present a detailed analysis of the dendritic and axonal morphology of excitatory neurons in layer 6B of the adolescent somatosensory rat barrel cortex and propose a classification scheme of neuronal subtypes present in this layer. Our data suggest that excitatory L6B neurons are an integral element of intra- and translaminar cortical signal processing.

Materials and Methods

Brain Slice Preparation

All experimental procedures were carried out in accordance to the German Animal Welfare Act and the guidelines of the Federation of European Laboratory Animal Science Association; the appropriate permission for sacrificing animals for brain slice experiments was obtained from the Northrhine-Westphalian Landesamt für Natur, Umwelt und Verbraucherschutz. Wistar rats (Charles River, either sex) aged 17–24 postnatal days (P17–24) were anesthetized with isoflurane (Delta Select) and decapitated. A series of 350-µm-thick brain slices of the somatosensory cortex were cut in cold extracellular solution using a vibrating microtome (HM 650 V, Microm). Slices were cut at an angle of 45–50° to the midline (Agmon and Connors 1991; Feldmeyer et al. 1999; Feldmeyer et al. 2006), incubated at room temperature (21–24 °C) in an extracellular solution with a low calcium and a high

magnesium concentration (i.e. 1 mM $CaCl_2$ and 4 mM $MgCl_2$) to minimize overall synaptic transmission.

Solutions

Slices were continuously superfused with an extracellular solution at a speed of 4–5 mL/min (in mM): 125 NaCl, 25 $NaHCO_3$, 2.5 KCl, 1.25 NaH_2PO_4, 1 $MgCl_2$, 2 $CaCl_2$, 25 glucose, and bubbled with 95% O_2 and 5% CO_2. The pipette (intracellular) solution contained (in mM): 135 potassium gluconate, 4 KCl, 10 HEPES, 10 phosphocreatine, 4 Mg-ATP, and 0.3 GTP (adjusted to pH 7.4 with KOH). The osmolarity of the solution was 290–300 mOsm. Biocytin (Sigma-Aldrich) was added at a final concentration of up to 5 mg/mL to the internal solution (see also Radnikow et al. 2012).

Identification of Neocortical Structures and L6B Neurons

Slices were placed in a submerged recording chamber and observed with an upright, fixed stage motorized microscope (BX51 WI, Olympus) fitted with 4× Plan/0.13 NA and 40× W/0.8 NA objectives. The lamination and the barrels of the neocortex are clearly visible at 20-fold magnification (Fig. 1*A1*). In acute brain slices, barrels can be identified as evenly spaced light hollows in neocortical layer 4 separated by dark narrow stripes (Agmon and Connors 1991; Feldmeyer et al. 1999; Land and Kandler 2002). L6B neurons were identified at 800-fold magnification (Fig. 1*A2*) under infrared light (IR) and differential interference contrast (DIC) optics (Dodt and Zieglgansberger 1990) using transmission bright-field video microscopy (Stuart et al. 1993).

Electrophysiological Recordings and Analysis

Whole-cell voltage- and current-clamp recordings from L6B neurons were made using patch-pipettes (5–9 MΩ) pulled from borosilicate glass capillaries (outer diameter 1.5 mm, inner diameter 0.9 mm; Hilgenberg). Neurons were randomly selected, patched, and filled with biocytin for at least 15–20 min. Signals were amplified using either an EPC 10 amplifier (HEKA Elektronik), filtered at 3 kHz and sampled at 1–10 kHz. Stimulation protocols were programmed using the "Patchmaster" software (HEKA Elektronik).

Neurons were not preselected based on their IR–DIC image or firing pattern. Only cells with a stable resting membrane potential (RMP) were used in this study. Twelve variables describing the active and passive electrophysiological properties (see Table 3) were measured for each neuron and analyzed using custom-written macros in Igor Pro 6 (WaveMetrics).

Histological Procedures and Morphological Reconstructions

After recording, slices were fixed at 4 °C for at least 12 h in 100 mM phosphate buffer solution (pH 7.4) containing 4% paraformaldehyde. Slices containing biocytin-filled neurons were processed using a modified protocol described previously (Lübke et al. 1996; Feldmeyer et al. 2006; Marx et al. 2012; Radnikow et al. 2012). Slices were incubated in 0.1% Triton X-100 solution containing avidin-biotinylated horseradish peroxidase (Vector ABC staining kit, Vector Lab. Inc.). The reaction was catalyzed with 3,3-diaminobenzidine as a chromogen under visual control until the dendritic and axonal arborization was clearly visible (Fig. 1*B*). Slices were then slowly dehydrated with ethanol and xylene and mounted on gelatinized object slides and embedded in Eukitt medium (Otto Kindler GmbH).

Subsequently, 3D reconstructions of the neurons were made with the NEUROLUCIDA® software (MicroBrightField; Fig. 1*C*; see also Glaser and Glaser 1990) using an Olympus BX61 microscope at a final magnification of 1000-fold. Only neurons with a clear labeling, minimal background staining, and with few visible transection of dendrites and axons were reconstructed. The contours of the pial surface, layer borders, and the barrels in layer 4 were also drawn. Reconstructions were aligned with respect to the pial surface and corrected for tissue shrinkage in all spatial dimensions (factor 1.1 in the *x*- and *y*-dimension, factor of 2.1 in the *z*-dimension) to obtain realistic neuronal morphologies (see also Marx et al. 2012). These 3D reconstructions provided the basis for the subsequent morphological analysis.

Morphological Data Analysis

For morphological data analysis NEUROEXPLORER® software (MicroBrightField) was used to conduct various morphological measurements to analyze the specific characteristics of somatodendritic and axonal structures. Furthermore, the distribution and percentage of dendrites and axons within cortical layers and barrel-related columns were determined. The width of the home barrel was defined using horizontal extent of the barrel and half of the septum to either side (cf. Helmstaedter et al. 2009a, 2009b, 2009c); its extension to the pial surface, and the white matter defined the barrel column. The localization of neurons in the barrel cortex was described with respect to the barrel column (trans- vs. intracolumnar) and the cortical lamination (trans- vs. intralaminar; infralaminar vs. superficial). Layer 6B is defined to be the local lamina (intralaminar). Layers 1–6A were described as superficial layers and the white matter as an infralaminar layer. All neuronal reconstructions with a total axon length ≤3000 µm were excluded from our analysis. The soma coordinates with respect to the superjacent barrels were used to superimpose reconstructions and for further analysis such as the construction of density maps. We used an unified cortical model that corresponds to an averaged neocortical lamination and barrel field of all 3D reconstructions.

Polar Plots

The neuronal polarity of each 3D reconstruction was calculated with NEUROEXPLORER® software using cubic spline smoothing. The dendritic and axonal length was averaged for each of the 120 "3° sectors" around the soma. Data were recalculated, plotted in angular

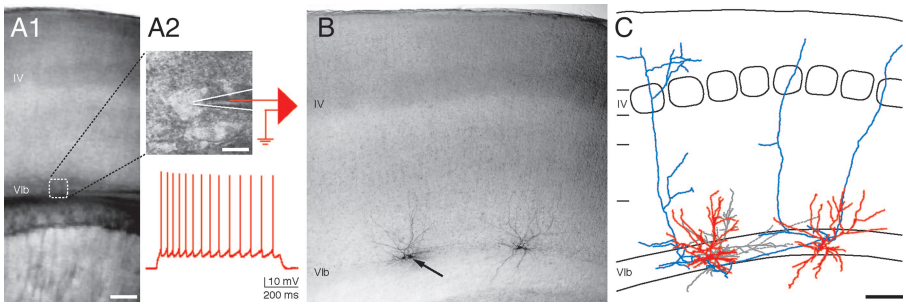

Figure 1. Patch-clamp recording, biocytin staining, and 3D reconstruction of L6B neurons. (*A1*) Transmission bright-field microscopic image of a thalamocortical brain slice under IR–DIC optics. (*A2*) Higher magnification image of the boxed region in (*A1*). The physiological properties of L6B neurons were recorded using whole-cell patch-clamp technique while simultaneously filling the cells with biocytin. The outline of the patch pipette is enhanced by white lines. (*B*) Brain slice processed for intracellular biocytin and embedded in Eukitt reveals the neocortical lamination, the barrels in layer 4 and the recorded neurons in layer 6B (×40). (*C*) 3D reconstruction of the neurons shown in (*B*). Dendrites are shown in red and axons in blue. A dye-coupled neuron (arrow in *B*) is presented in gray. Layer borders and the barrel fields were also drawn. Scale bars in (*A1*) 300 µm; (*A2*) 20 µm; and (*B*, *C*) 300 µm.

subdivision around the soma, and polar plots were made with Grapher software (GoldenSoftware). The radian depicts degree in angles (°) with 0° towards the pial surface, 90° towards the posterior-median axis, 180° towards the white matter, and 270° towards the anterior-lateral axis.

Dendritic and Axonal Density Maps

Maps of the dendritic and axonal "length density" were constructed using the computerized 3D reconstructions (Lübke et al. 2003; Helmstaedter and Feldmeyer 2010). All reconstructions from a single cell type were superimposed and aligned to the barrel center with respect to their relative soma positions. The dendritic and axonal length of all neurons was measured in a 50 µm × 50 µm Cartesian grid, yielding a raw density map of the dendritic arborization and axonal collateralization by using the open-source software NEURON (http://www.neuron.yale.edu). Spatial low-pass filtering of these maps was performed with a Gaussian kernel ($\sigma = 50$ µm) and converted to a continuous density function using bicubic interpolation in Mathematica (Wolfram Research).

Cluster Analysis and Statistics

All data were presented as average ± standard error of the mean (SEM). Statistical analyses were performed using either an unpaired independent *t*-test or a one-way multiple variance analysis (i.e. analysis of variance [ANOVA]). Statistical significance (α) was set at least to $\alpha = 0.05$.

To avoid the inclusion of highly correlated variables into the cluster analysis (CA) we performed a principal component analysis (data not shown). We found that some morphological parameters were indeed highly correlated (e.g. soma properties such as surface area and volume, length, and number of dendrites, nodes, endings, etc.). We made an effort to find additional variables that can distinctly classify neuronal morphology of L6B neurons (e.g. the dendritic orientation such as the columnar and laminar distribution of dendritic and axonal structures). Using this approach, we were able to exclude all variables from the CA which were highly correlated or showed a low degree of variance thereby avoiding double weighting or misinterpretation by the CA.

In total, eight somatodendritic and five axonal morphological parameters were chosen, normalized and used for an unsupervised CA (see Table 1). Furthermore, seven physiological parameters (action potential [AP] half-width, firing frequency per 100 pA, membrane time constant [τ_M], inter-spike interval [ISI], adaptation ratio, AP, and after hyperpolarization [AHP] amplitudes) were added to the CA. This facilitated a clear separation of the interneuron control group from the excitatory neurons. For the CA, distances were measured as Euclidean and Ward's method (Ward 1963) was used for calculating the linkage distance, that is the degree of variance among the observed morphological parameters. In brief, the linkage step leading to the maximum increase in linkage distance was used for the cutoff representing three individual clusters. The cutoff was determined using Thorndike's procedure (Thorndike 1953; Cauli et al. 2000).

Table 1
Morphological and physiological parameters of L6B neurons that were used for the CA

Dendritic morphology	Axonal morphology	Physiology
Total dendrite length (µm)	Total axon length (≥3000 µm)	AP half-width (ms)
Dendritic branching frequency (nodes/100 µm)	Axonal branching frequency (nodes/100 µm)	Firing frequency per 100 pA
		τ_M (ms)
Max. cortical dendritic field span (µm)	Max. cortical axonal field span (µm)	Min. ISI (ms)
Laminar distribution of dendrites (superficial vs. local/infralaminar)	Laminar distribution of axons (superficial vs. local/infralaminar)	Adaptation ratio
		AP amplitude (mV)
Columnar distribution of dendrites (intracolumnar vs. transcolumnar)	Columnar distribution of axons (intracolumnar vs. transcolumnar)	AHP amplitude (mV)
Spiny/spineless dendrites		
Main dendrite (apical or "apical"-like)		
Orientation of main dendrites		

Results

CA and Neuronal Cell Classification

Layer 6B is visible as a small dark zone of 191.5 ± 53.3 µm width ($n = 93$) that lies between the more superficial and wider layer 6A and the deeper white matter. In our study we found layer 6 to be clearly subdivided into two separate laminae of which the more superficial sublamina 6A occupied on average 65.5 ± 3.9% and the deeper sublamina 6B 34.5 ± 3.9%; values that are roughly comparable with those in recent publications (Kumar and Ohana 2008; Meyer et al. 2010; Oberlaender et al. 2011; Perrenoud et al. 2012).

For the classification of the different L6B neuronal subtypes, 155 neurons were randomly patched in acute slices of the adolescent (P17–24) primary somatosensory barrel cortex of the rat. The average distance of L6B neurons from the white matter was 107.4 ± 43.9 µm. Their distance relatively to the width of the entire layer 6 was in the lower third of this lamina (Supplementary Fig. S1).

L6B neurons were recorded in whole-cell voltage- and current-clamp mode and simultaneously filled with biocytin (Fig. 1). Only neurons with an excellent labeling of the somatodendritic and axonal domain and with minimal background staining as well as a stable RMP were used for physiological and morphological data analyses. Using acute brain slices leads often to a truncation of long axon collaterals. To overcome this problem and to allow a more reliable comparison with in vivo studies, we applied a further criterion and excluded all neurons with a total axon length ≤3000 µm (i.e. a high transection of dendrites and especially axons). Further, we excluded neurons with a relative neocortical position which was not clearly within layer 6B from the data pool. The morphological and electrophysiological data for this study were obtained from a total of 93 reconstructed neurons (i.e. 87 excitatory and 6 inhibitory neurons). Neurons were classified as excitatory when their dendritic spine density was high, a generally accepted criterion for glutamatergic neurons (e.g. Feldman and Peters 1978; Connors and Gutnick 1990). While some GABAergic interneurons also possess dendritic spines, their density was substantially lower than that of excitatory neurons. In addition, these interneurons had also clearly distinct AP firing patterns (McCormick et al. 1985; Kawaguchi and Kubota 1993; Thomson et al. 1996; Kawaguchi and Kubota 1997; see also Petilla terminology by Ascoli et al. 2008).

The dendrogram that resulted from the CA for the L6B neurons (Fig. 2*A*) shows three distinct clusters of neuronal cell types designated as: (C1) neurons with a distinct apical dendrite towards the pial surface, that is, pyramidal neurons; (C2) neurons with a prominent "apical"-like dendrite not towards the pial surface; and (C3) multipolar neurons without any preferential dendrite orientation. The second neuronal cell cluster with a prominent "apical"-like dendrite could be further subdivided, identifying three subclusters termed (C2a) inverted, (C2b) "tangentially" oriented, and (C2c) "horizontally" oriented neurons. Furthermore, two subcategories of L6B pyramidal cells were found, one of which had a more barrel-column confined axon while that of the other had

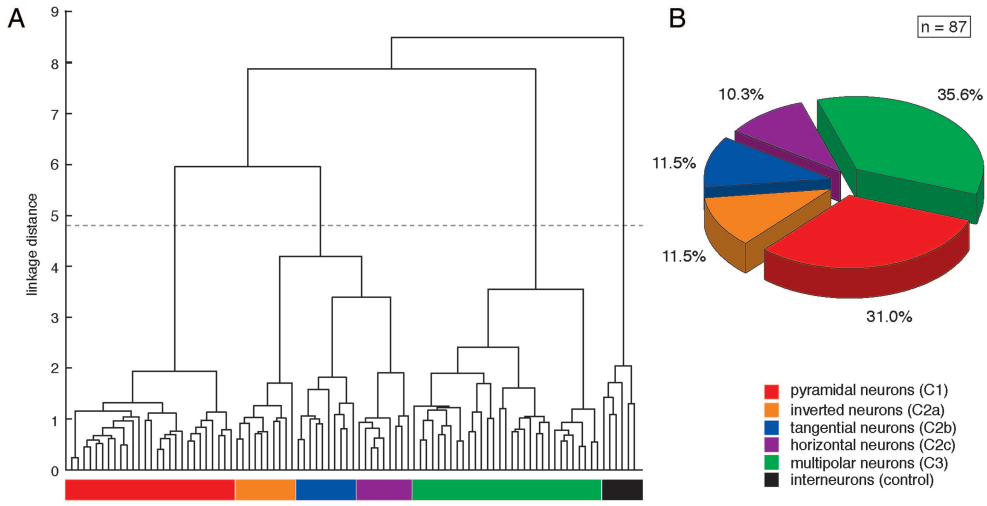

Figure 2. CA of L6B neurons. (*A*) The linkage dendrogram for the unsupervised CA of morphological and functional parameters of L6B neurons are listed in Table 1. L6B interneurons have been included in the analysis as controls and were clearly separated from the excitatory L6B neurons. The *x*-axis represents individual cells, and the *y*-axis represents the average Euclidean within-cluster linkage distance; the dashed line indicates the cutoff as determined by Thorndike's procedure (Thorndike 1953). Three distinct main clusters could be defined: (C1) neurons with a distinct apical dendrite towards the pial surface, (C2) neurons with a main "apical"-like dendrite not towards the pial surface, and (C3) multipolar neurons without any preferential orientation. Cluster C2 was further subdivided into 3 subclusters based on the orientation of the dominant "apical"-like dendrite. Five excitatory L6B neuron types were designated as C1: pyramidal neurons (red), C2a: inverted neurons (orange), C2b: "tangentially" oriented neurons (blue), C2c: "horizontally" oriented neurons (violet), and C3: multipolar neurons (green). (*B*) The pie chart demonstrating the percentage of each excitatory L6B cell type with 27 pyramidal neurons (31.0%), 10 inverted neurons, 10 "tangential" neurons (both 11.5%), 9 "horizontal" neurons (10.3%), and 31 multipolar neurons (35.6%).

projections over a much larger cortical area. In summary 27 regular pyramidal neurons (31.0%), 10 inverted neurons, 10 "tangential" neurons (both 11.5%), 9 "horizontal" neurons (10.3%), and 31 multipolar neurons (35.6%) could be assigned to the five neuronal cell types in neocortical layer 6B (Fig. 2*B*). An examplary reconstruction of each L6B cell type is presented in Figure 3. For the visualization of the 3D geometry, each representative example is shown in its *xy*-dimension (Fig. 3*A–E1*), *yz*-dimension (Fig. 3*A–E2*), and *xz*-dimension (Fig. 3*A–E3*), respectively.

Morphological Classification

Quantitative parameters describing the dendritic and axonal morphology show an overall significant difference ($P < 0.05$) between all five neuronal cell types in layer 6B (see Table 2). The only exception was the percentage of the axon found in superficial layers (i.e. layers 5 to 2/3; $P > 0.759$) and the axonal branching frequency ($P > 0.084$). Barrel dimensions, layer borders, and the relative neuronal soma positions within a barrel-related column were also not significantly different ($P > 0.05$).

Cluster C1: Neurons with an Apical Dendrite Oriented Towards the Pial Surface

Pyramidal L6B Neurons

The first cluster (C1) comprises 27 pyramidal neurons (Figs 3*A1–3* and 5*A1,3*). These neurons have a thick apical main dendrite that was clearly discernible from all other dendrites (i.e. basal dendrites). Their average initial diameter of the main apical trunk (i.e. the maximal diameter at 10 µm distance from the soma) was 4.5 ± 1.1 µm compared with a mean diameter of 1.0 ± 0.2 µm of the basal dendrites. Apical dendrites project directly towards the pial surface at a polar plot angle ~0° (Fig. 4*A1*). L6B pyramidal neurons have a total dendrite length of 5096 ± 1058 µm, 32.6 ± 6.2 nodes, a dendritic branching frequency of 0.07 ± 0.01 nodes/100 µm, and a field span of 336 ± 120 µm. Their dendrites reside largely in the home barrel column (89.6 ± 9.2%) as indicated by the dendritic length density map of this L6B neuron type (Fig. 5*A1,2*). Some L6B pyramidal neurons have apical dendrites that extend into the more superficial layers 5A and 5B ($n = 18$) but not further than layer 4; others have only short apical dendrites terminating in sublamina 6A ($n = 9$). L6B pyramidal cells can be differentiated also on the basis of their apical tufts. Some apical dendrites terminate in elaborate or moderate tufts ($n = 16$) while others are virtually untufted ($n = 12$). Short pyramidal neurons are generally untufted whereas large and medium pyramidal neurons have at least a moderate apical tuft. A few oblique dendrites are present in lower layer 5B and in upper layer 6A, whereas basal dendrites in lower layer 6A and the entire laye 6B show many bifurcations and give rise to higher-order dendritic branches (Fig. 7*A1*, *B1* and Supplementary Fig. S2).

The total axon length of L6B pyramidal neurons is about 4639 ± 1561 µm with 13.3 ± 5.2 nodes and an axonal branching frequency of 0.03 ± 0.01 nodes/100 µm. The axonal polar plot for L6B pyramidal neurons shows a main orientation towards the pial surface (polar plot angles: 0 ± 30°; Fig. 4*A2*). Furthermore, these neurons have a high axonal length density within their home cortical column and throughout layers 5 and 6 (Fig. 5*A3,4*).

Cluster C2: Neurons with an "Apical"-Like Dendrite Oriented not Towards the Pial Surface

Inverted L6B neurons

Ten inverted L6B neurons belong to the first subgroup of cluster C2 (C2a; Figs 3*B1–3* and 5*B1,3*). They show an atypically oriented thick "apical"-like main dendrite which always extends from the basal site of the soma and directly

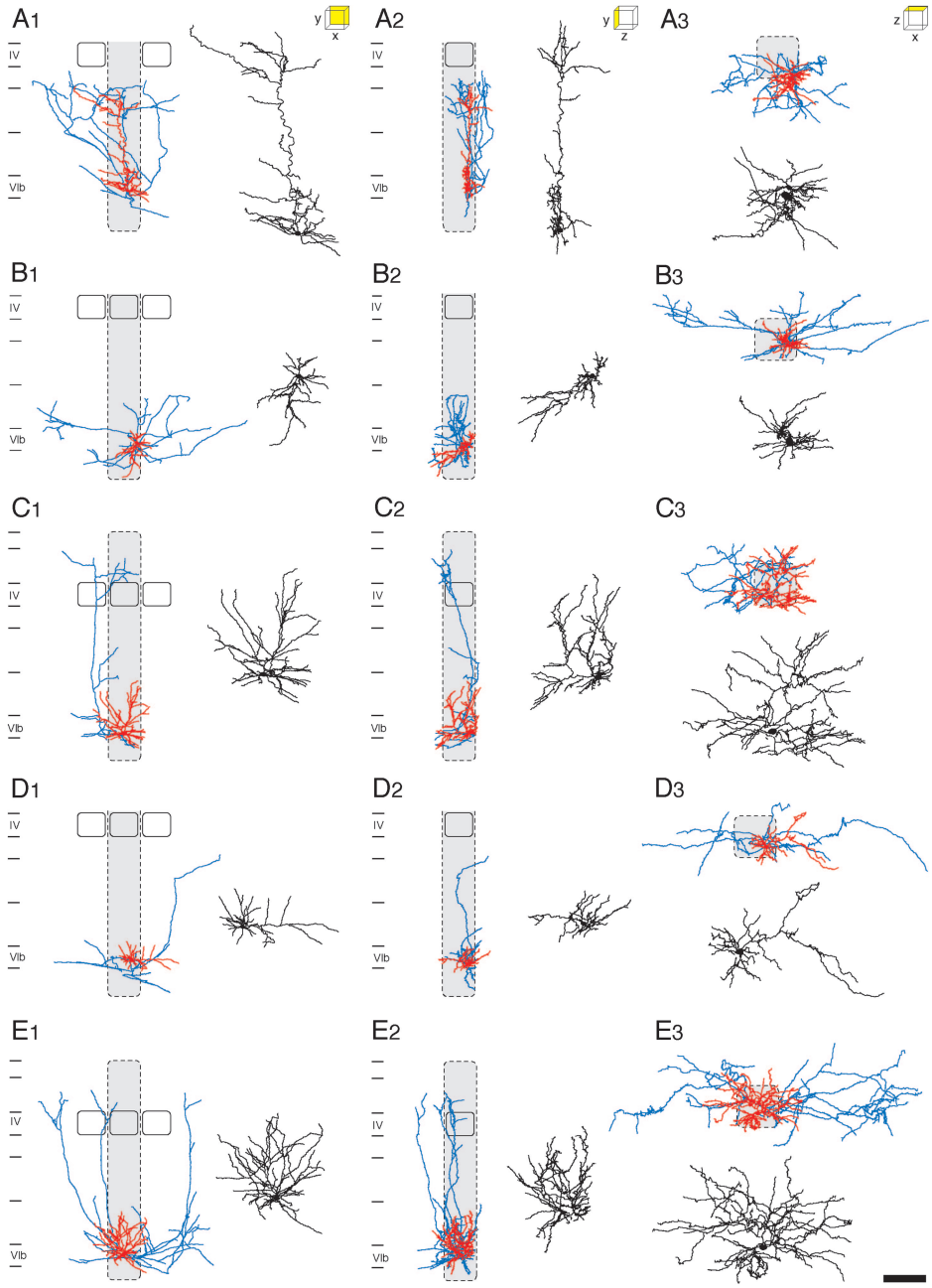

Figure 3. Examples of individual excitatory L6B neurons of each of the five subgroups. A representative reconstruction for a (*A*) pyramidal neuron, (*B*) inverted neuron, (*C*) "tangentially" oriented neuron, (*D*) "horizontally" oriented neuron, and (*E*) multipolar neuron is shown from three different angles: (1) *xy*-, (2) *yz*- (3) and *xz*-direction (3D cubes in *A1–3*). The nomenclature (*A*, *B*, *C*, *D*, *E*) is in accordance with the clustering in Figure 2 (i.e. cluster C1, C2a, C2b, C2c, and C3). Note the different dendritic and axonal projection pattern of all five L6B cell types. Dendrites are shown in red, axons in blue, respectively. A two-fold magnification of each somatodendritic structure is represented in black. Neuronal reconstructions are shown in their relative cortical positions. Scale bar in *A1–E2*: 300 μm; *A3–E3*: 200 μm. Scale bar for the somatodendritic magnification in *A1–E2*: 150 μm; *A3–E3*: 100 μm.

projects towards the white matter. Inverted neurons show different morphological shapes and have a total dendritic length of 4630 ± 972 μm, 23.2 ± 6.0 nodes, and a branching frequency of 0.05 ± 0.01 branches/100 μm. The dendrites of inverted L6B neurons are predominantly confined to the barrel column (78.5 ± 10.8%) and have an average dendritic field span of 478 ± 134 μm. The polar plot and density map clearly show that the dendritic domain of inverted L6B neurons is mainly oriented towards and into the white matter (polar plot angles: 180 ± 60°; Figs 4*B1* and 5*B1*) with a few dendrites projecting into sublamina 6A but not further.

The total axon length is 7469 ± 3172 μm with 23.6 ± 12.1 bifurcating nodes and an axonal branching frequency of 0.03 ± 0.01 branches/100 μm. Both the polar plot and density map of inverted neurons show a rather distinct axonal orientation pattern. Axons are mainly horizontally oriented with a high degree of collateralization. The majority of the axonal domain of these neurons resides in layer 6B (86.2 ± 16.7%) and run mostly in the horizontal direction (polar plot angles: 90 ± 30° or 270° ± 30°; Fig. 4*B2*). A few collaterals projecting to layer 6A and the white matter are also present. The average axonal field span for this cell type is 1304 ± 714 μm (Fig. 5*B3,4*, *B4*).

Table 2
Morphological parameters of L6B neuronal cell types

Morphological parameters	Pyramidal	Inverted	Tangential	Horizontal	Multipolar	*P* value
n	27	10	10	9	31	—
Distance soma – white matter (μm)	112 ± 53	128 ± 45	130 ± 49	106 ± 59	93 ± 39	0.157
Barrel width (μm)[a]	224 ± 46	245 ± 33	246 ± 556	253 ± 41	232 ± 60.0	0.506
Total dendrite length (μm)	5096 ± 1059	4630 ± 973	7006 ± 2024	5047 ± 2490	7666 ± 2818	1.55E−05
No. of dendritic nodes	32.6 ± 6.2	23.2 ± 6.0	29.1 ± 10.0	26.0 ± 12.4	37.8 ± 16.6	5.79E−03
Dendritic branching frequency (nodes/100 μm)	0.06 ± 0.01	0.05 ± 0.01	0.04 ± 0.01	0.05 ± 0.01	0.05 ± 0.01	6.94E−09
Avg. dendritic field span (μm)	336 ± 120	478 ± 134	491 ± 123	593 ± 201	559 ± 137	2.47E−07
Superficial dendrite length (μm)	2783 ± 1002	286 ± 505	3267 ± 1893	1818 ± 2112	3839 ± 2264	5.79E−06
Superficial dendrite percentage	56.2 ± 18.2	6.3 ± 11.9	44.2 ± 18.8	27.0 ± 22.7	46.1 ± 21.3	1.16E−08
Local/infralaminar dendrite length (μm)	2207 ± 1026	4344 ± 1104	3740 ± 1291	3229 ± 723	3827 ± 1742	3.80E−05
Local/infralaminar dendrite percentage	43.8 ± 18.2	93.7 ± 11.9	55.8 ± 18.8	73.0 ± 22.7	53.9 ± 21.3	1.16E−08
Columnar dendrite length (μm)	4560 ± 1010	3582 ± 689	4681 ± 1311	3089 ± 1231	4929 ± 2024	8.87E−03
Columnar dendrite percentage	89.6 ± 9.2	78.5 ± 10.8	67.7 ± 15.8	63.7 ± 10.2	65.1 ± 11.5	5.34E−12
Transcolumnar dendrite length (μm)	536.0 ± 505	1048 ± 592	2325 ± 1237	1958 ± 1331	2737 ± 1397	4.62E−10
Transcolumnar dendrite percentage	10.4 ± 9.2	21.6 ± 10.8	32.3 ± 15.8	36.3 ± 10.2	35.0 ± 11.5	5.34E−12
Total axon length (μm)	4639 ± 1562	7469 ± 3173	8777 ± 4036	4538 ± 1220	7094 ± 3930	8.71E−04
No. of axonal nodes	13.3 ± 5.2	23.6 ± 12.1	26.9 ± 22.0	14.0 ± 4.9	21.6 ± 12.1	4.78E−03
Axonal branching frequency (nodes/100 μm)	0.03 ± 0.01	0.03 ± 0.01	0.03 ± 0.01	0.03 ± 0.01	0.03 ± 0.01	0.759
Avg. axonal field span (μm)	686 ± 383	1305 ± 714	831 ± 490	904 ± 279	939 ± 337	4.15E−03
Superficial axon length (μm)	2588 ± 1591	1274 ± 1695	2959 ± 1478	1740 ± 435	3095 ± 2609	0.084
Superficial axon percentage	53.2 ± 21.7	13.8 ± 16.7	34.6 ± 15.2	40.7 ± 13.9	42.4 ± 19.3	1.27E−05
Local/infralaminar axon length (μm)	2051 ± 879	6195 ± 2234	5818 ± 3386	2798 ± 1235	4000 ± 2343	2.32E−07
Local/infralaminar axon percentage	46.8 ± 21.7	86.2 ± 16.7	65.4 ± 15.2	59.3 ± 13.9	57.60 ± 19.3	1.27E−05
Columnar axon length (μm)	2479 ± 1123	2817 ± 1350	4222 ± 1795	1910 ± 558	2701 ± 1236	1.41E−03
Columnar axon percentage	54.1 ± 19.1	39.7 ± 12.8	49.6 ± 12.2	42.4 ± 7.7	41.9 ± 17.2	0.033
Transcolumnar axon length (μm)	2160 ± 1241	4652 ± 2618	4556 ± 2614	2628 ± 883	4393 ± 3304	3.33E−03
Transcolumnar axon percentage	46.0 ± 19.1	60.3 ± 12.8	50.4 ± 12.2	57.6 ± 7.7	58.1 ± 17.2	0.033

[a]The width of the home barrel was defined using horizontal extent of the barrel and half of the septum to either side (cf. Helmstaedter et al. 2009a, 2009b, 2009c).

Some collaterals of the inverted L6B neurons span well over 5 barrel columns.

"*Tangentially*" *Oriented L6B Neurons*

The second subgroup of C2 comprises 10 "tangential" neurons with a thick main dendrite extending obliquely from the soma (Figs 3*C1–3* and 5*C1,3*). "Tangentially" oriented neurons have a high total dendrite length of 7006 ± 2024 μm, 29.1 ± 10.0 nodes, and a dendritic branching frequency of 0.04 ± 0.01 branches/100 μm. Their maximal dendritic field span is 491 ± 123 μm. The polar plot shows a preferential dendritic projection tangentially towards the pial surface (polar plot angles: 45 ± 30° or 315 ± 30°; Fig. 4*C1*). Dendrites terminate mainly in the superficial layers 6A and 6B with highly variable dendritic projection patterns. However, some dendrites ascend up to lower layer 5B.

The total axon length of this L6B neuron type is 8777 ± 4036 μm with 26.9 ± 22.0 nodes, an axonal branching frequency of 0.03 ± 0.01 branches/100 μm, and an axonal field span of 831 ± 490 μm. The axon polarity has a moderate horizontal orientation, but is strongly oriented towards the pial surface (Fig. 4*C2*). The axonal density map for "tangentially" oriented L6B neurons indicates that these neurons may innervate other L6B neurons from the home and adjacent barrel columns (Fig. 5*C3,4*) and neurons as well in superficial layers 5 and 6. The ratio of intracolumnar and transcolumnar axon is almost identical with 49.6 vs 50.3 ± 12.2%.

"*Horizontally*" *Oriented L6B Neurons*

The third subgroup of C2 comprises 9 neurons with a "horizontally" oriented main dendrite extending from the posterior-medial or anterior-lateral site of the soma (C2c; Figs 3*D1–3* and 5*D1,3*). "Horizontal" neurons have a total dendritic length of 5047 ± 2490 μm, 26.0 ± 12.4 nodes, and a dendritic branching frequency of 0.05 ± 0.01 branches/100 μm. The average dendritic field span is 593 ± 201 μm. The polar plot shows a common horizontal dendritic orientation in sublamina 6B (polar plot angles: 90 ± 15° or 270 ± 15°; Fig. 4*D1*). More than two-thirds of the dendritic domain of "horizontal" L6B neurons (73.0 ± 22.7%) resides in sublamina 6B and the subjacent white matter with some dendritic branches projecting into neighboring barrel columns. A few "horizontal" L6B neurons ($n = 3$) also have a high dendritic arborization in upper lamina 6A due to the presence of a secondary dendrite.

The total axon length is 4538 ± 1220 μm with 14.0 ± 4.9 nodes, an axonal branching frequency of 0.03 ± 0.01 branches/100 μm, and a field span of 904 ± 279 μm. The axonal polarity is comparable with that of the dendrites, but with a slight orientation towards the pial surface (Fig. 4*D2*). A substantial fraction of their axon projects across several barrel columns and thus more than half of the total axon length (57.6 ± 7.7%) is transcolumnar. Only few axon collaterals ascend to layer 5A but not beyond. The axonal density map shows a prominent projection in the home and neighboring barrel columns (Fig. 5*D3,4*) which is clearly a distinct feature of this L6B neuron type.

Cluster C3: Multipolar Neurons Without any Preferential Dendritic Orientation

Multipolar L6B Neurons

Cluster C3 comprises 31 multipolar neurons with no dominant apical or "apical"-like main dendrite (Figs 3*E1–3* and 5*E1,3*), but many long dendrites running in various directions. They have the highest total dendritic length of all L6B neuron types (7666 ± 2818 μm) with 37.8 ± 16.6 nodes and a dendritic branching frequency of 0.05 ± 0.01

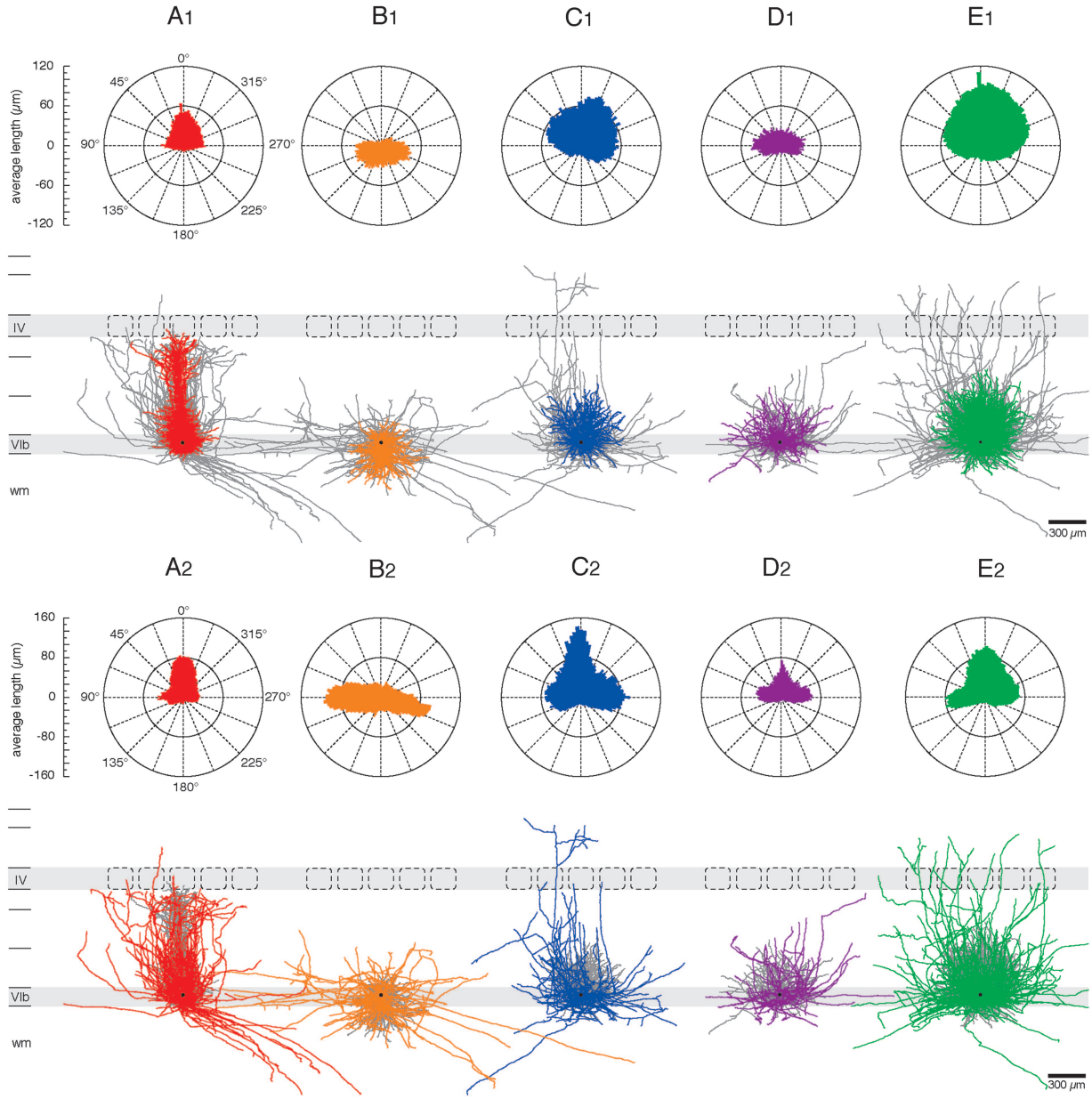

Figure 4. Dendritic and axonal polarity of excitatory L6B neuron types. The polar plots represent the characteristic dendritic and axonal orientation of (*A1, A2*) pyramidal neurons, (*B1, B2*) inverted neurons, (*C1, C2*) "tangentially" oriented neurons, (*D1, D2*) "horizontally" oriented neurons, and (*E1, E2*) multipolar neurons. The average dendritic and axonal length of all 3D reconstructions was calculated for 120 "3° sectors" with the aid of NEUROEXPLORER® using cubic spline smoothing and plotted in angular subdivision around the soma. The radian depicts degree in angles (°) and is encoded with 0° towards the pial surface, 90° towards the posterior-median axis, 180° towards the white matter (wm), and 270° towards the anterior-lateral axis, respectively. All neuronal cell reconstructions are superimposed and soma-centered. Individual cell somata are presented by black dots. The color code is identical to that given in Figure 2. Axons in *A1–E1* and dendrites in *A2–E2* are presented in dark gray. Scale bars = 300 μm.

branches/100 µm. Multipolar neurons have a broad dendritic domain within neocortical layers 5 and 6 with dense ascending projections into sublamina 6A and some branches descending towards the white matter. Their dendrites project across the barrel-related columns with an average dendritic field span of 559 ± 137 µm. The dendritic polar plot as well as the density map show a wide, almost circular dendritic field without any preferential orientation (Figs 4*E1* and 5*E2*).

The axons of multipolar neurons project mainly within layer 6 with a few collaterals extending into lower layer 5B. The total axon length is 7094 ± 3930 µm with 21.6 ± 12.1 nodes and an axonal branching frequency of 0.03 ± 0.01 branches/100 µm. The axonal polarity is comparable with those of "tangential" neurons with predominant axonal projections in horizontal directions and to the pial surface (Fig. 4*E2*). Multipolar neurons have a high axonal length density covering neocortical layers 5 and 6 to a high degree (Fig. 5*E3,4*). The axonal domain of multipolar L6B neurons is confined to the lower layers of the somatosensory cortex; however some collaterals ascend even up to layers 2/3. The average axonal field span is about 939 ± 337 µm. Thus, the axons of multipolar L6B neurons project over five or more barrel-related columns.

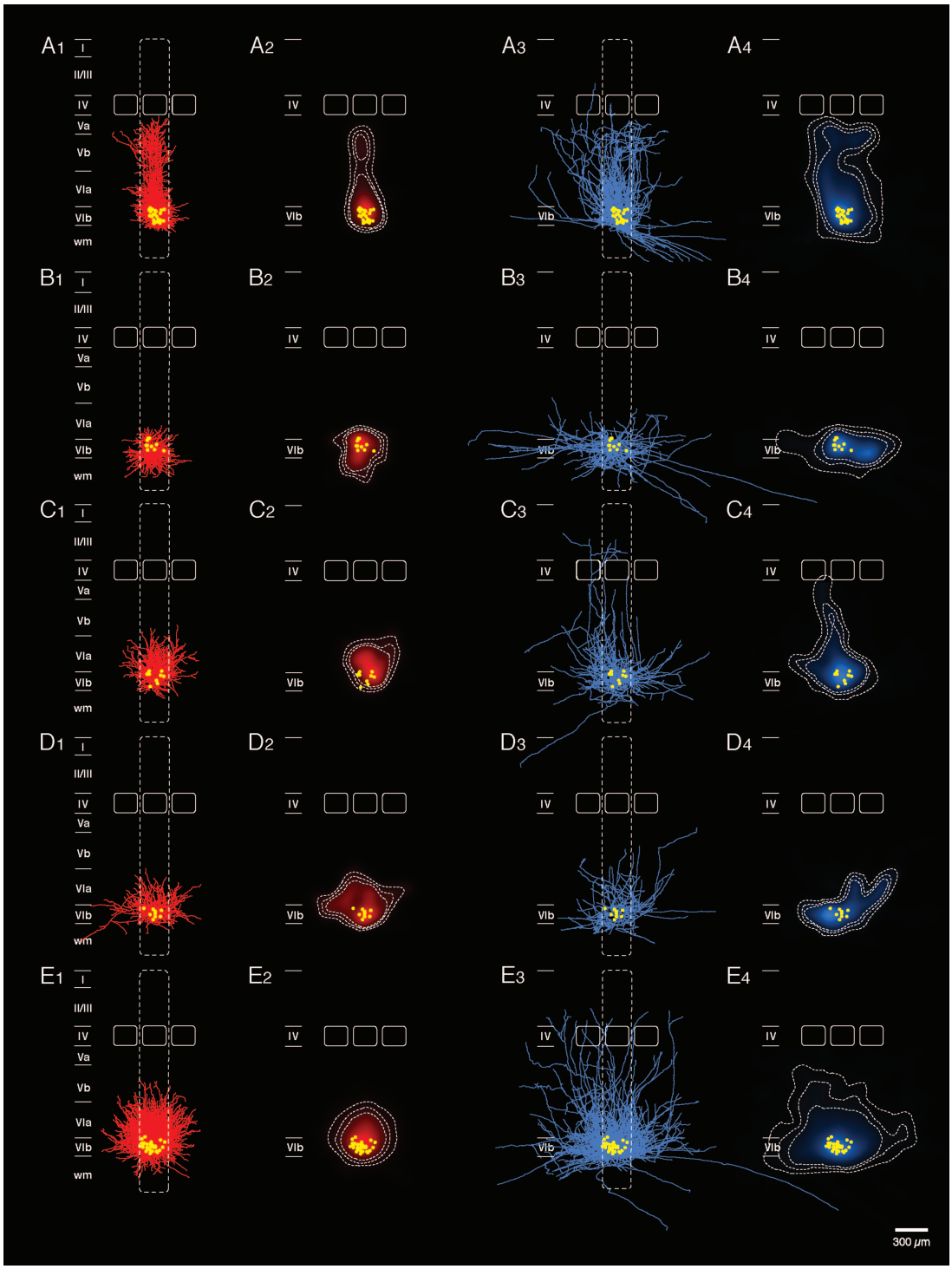

Figure 5. Density maps of excitatory L6B neuron types. Reconstruction overlays and density maps of each L6B neuron type are shown for (*A*) pyramidal neurons, (*B*) inverted neurons, (*C*) "tangentially" oriented neurons, (*D*) "horizontally" oriented neurons, and (*E*) multipolar neurons. All dendritic and axonal reconstructions are superimposed with respect to the center of the home barrel column. Barrels in layer 4 are represented as white rectangles. The white contour lines superimposed on the density maps (in *A2,4, B2,4, C2,4, D2,4, E2,4*) enclose 70%, 80%, and 90% of the integrated dendritic and axonal density length, respectively. Dendrites and dendritic density maps are shown in red, axons and axonal density maps in blue. Individual cell somata are presented by yellow dots. The nomenclature *A*, *B*, *C*, *D*, *E* is in accordance with the clustering in Figure 2 (i.e. C1, C2a, C2b, C2c and C3). Scale bar = 300 μm.

Physiological Properties of Excitatory and Inhibitory L6B Neurons

All neuronal cell types in sublamina 6B presented here exhibit spines on their dendritic branches and show a regular excitatory firing pattern. Apart from these spiny L6B neurons a few interneurons ($n = 6$) have been analyzed and added as a control group. Passive and active firing properties of the different types of L6B neurons were analyzed by voltage recordings in response to de- and hyperpolarizing current injections. Electrophysiological recordings from excitatory L6B

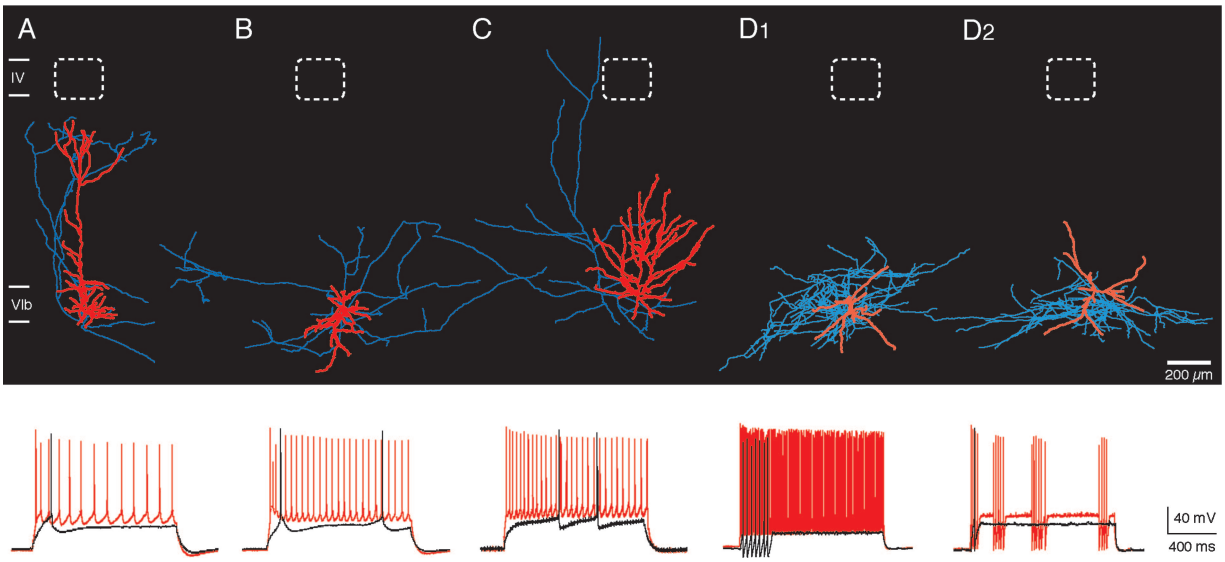

Figure 6. Morphological and physiologically distinct cell types of L6B neurons. Excitatory neurons have like interneurons a broad variety in their physiological properties. (*A*) An example of a 3D reconstruction of a pyramidal neuron with its appropriate firing pattern is shown. The electrophysiological traces correspond to the voltage respond to current injections in whole-cell current-clamp mode. The black trace shows the initial firing at low current injection. A full spike train at high current injection is illustrated by the red trace. Pyramidal neurons with a prominent thick apical dendrite show a RS pattern with high adaptation ratios (0.67 ± 0.11; $P < 0.00164$; see Table 3). (*B*) Inverted neurons have a higher firing frequency (19.7 ± 4.6 spikes/100 pA; $P < 0.013$) and a lower adaptation ratio than pyramidal neurons. Both pyramidal and inverted L6B neurons showed AP doublets or triplets at the beginning of the spike train but were absent in all other excitatory L6B neuron types. (*C*) Multipolar neuron with its appropriate firing pattern. Multipolar, "tangential," and "horizontal" neurons show a vast range of firing patterns; however, a common feature is their low adaptation ratio at higher current injections (0.5 ± 0.2; $P < 0.044$). Multipolar neurons have the longest ISI among all excitatory cell types (107.4 ± 74.0; $P < 0.0078$). Different types of interneurons were also found in layer 6B, for example: (*D1*) a continuously firing FS interneuron and (*D2*) a FS stuttering interneuron. All neuronal reconstructions are presented with their relative cortical position and have at least a total axon length ≥6000 μm (for interneurons ≥18 000 μm). The description for AP firing trains and the color code for morphological reconstructions in *A* applies also to *B*, *C*, *D1*, *D2*. Scale bar: 200 μm.

neurons with a stable RMP all show a regular spiking (RS) pattern following the injection of a suprathreshold depolarizing current (Fig. 6*A–C*). No significant difference in the RMP ($P > 0.13$), AP half-width ($P > 0.075$), and AHP ($P > 0.299$) were observed between the different excitatory L6B neuron types as defined here (see Table 3; *P* values calculated by a one-way ANOVA). For the other passive and active electrophysiological properties, differences in the mean values were observed but this was not consistent for a specific neuronal cell type. We recorded also from a few L6B interneurons. These interneurons could be tentatively classified as continuously fast-spiking (FS; Fig. 6*D1*), stuttering FS interneurons (Fig. 6*D2*), and adapting interneurons (not shown). These L6B interneurons observed here had smooth, spineless dendrites. They showed a very sharp and fast AHP which resulted in FS AP firing trains. Their AP firing frequency is much higher than that of the excitatory L6B neurons (52.1 ± 20.7 spikes/100 pA vs. 16.2 ± 6.7 spikes/100 pA; $P < 0.00849$), while the AP half-width (0.28 ± 0.04 ms vs. 1.11 ± 0.35 ms; $P < 0.0000648$), ISI (16.2 ± 12.2 ms vs. 81.9 ± 52.5 ms; $P < 0.00306$), and τ_M were significantly shorter (6.0 ± 3.8 ms vs. 16.4 ± 4.9 ms; $P < 0.00000187$). In summary, L6B interneurons could be clearly distinguished from the L6B excitatory neurons based on these functional parameters (see also Perrenoud et al. 2012).

Intracolumnar and Transcolumnar Pyramidal Cells

In an effort to further classify excitatory L6B neurons, we investigated the morphological characteristics of the axonal domain of L6B pyramidal cells in more detail. We were able to identify two distinct pyramidal subtypes in layer 6B (Fig. 7) based on their maximal axonal field span in the neocortex; the portion of the axon located in the white matter was omitted from this analysis. Ten pyramidal neurons could be designated as intracolumnar pyramidal cells (iPC; light blue axon; Fig. 7*A1,2*), whereas 17 pyramidal neurons were described as transcolumnar pyramidal cells (tPC; green axon; Fig. 7*B1,2*). The scatter plot reveals that there is no correlation between the axonal field span and the total axon length suggesting that this grouping is independent of the axonal length and hence not a truncation artifact. We have found pyramidal neurons with a high axon length and a broad axonal field span as well as neurons with a high axon length and a small axonal field span, respectively (Fig. 7*C1*).

There is a highly significant difference ($P < 0.001$) in their maximal axonal field span (iPCs: 373 ± 78 μm vs. tPCs: 870 ± 371 μm; Fig. 7*C2*), but no significant difference ($P > 0.1$) in the total axon length of iPCs (4190 ± 1041 μm) and tPCs (4903 ± 1775 μm; Fig. 7*C3*), respectively. A comparison of the axonal orientation reveals a similar projection towards the pial surface, but in a much broader polarity pattern for tPCs (not shown). The axons of iPCs are largely confined to a barrel-related column with 69.5 ± 20.4% (Fig. 7*A2*), in particular at the level of layer 5. In contrast, tPC axons project into the neighboring barrel columns at the level of layer 5 and extend over an even wider cortical area in layer 6 (Fig. 7*B*). Only 45.0 ± 11.3% of the tPC axons reside in the home barrel column (Fig. 7*B2*), a value that is significantly different from that of iPC axons ($P > 0.01$). In addition, at least some of the tPCs possess long-range axon collaterals that project over several barrels (up to 1000 μm) and can be seen to enter the secondary somatosensory cortex (S2), a feature that has not

Table 3
Selected active and passive electrophysiological properties of L6B neurons

Physiological parameters	Pyramidal	Inverted	Tangential	Horizontal	Multipolar	*P* value	Excitatory	Inhibitory	*P* value
n	27	10	10	9	31	–	87	6	–
Passive properties									
RMP (mV)	−69.9 ± 3.7	−68.1 ± 2.8	−72.3 ± 3.4	−70.0 ± 6.2	−71.8 ± 4.5	0.13	−70.7 ± 4.3	−66.1 ± 4.0	0.023
Input resistance (MΩ)	232.8 ± 60.6	269.4 ± 95.3	209.7 ± 81.4	256.5 ± 117.3	178.1 ± 75.3	7.01E−03	217.3 ± 84.4	192.6 ± 121.0	0.501
τ_M (ms)	17.6 ± 3.7	19.7 ± 4.6	14.9 ± 3.9	17.7 ± 5.2	14.5 ± 5.4	0.013	16.4 ± 4.9	6.0 ± 3.8	1.87E−06
Active properties									
AP half-width (ms)	1.00 ± 0.29	1.28 ± 0.41	1.10 ± 0.21	1.34 ± 0.58	1.06 ± 0.29	0.075	1.11 ± 0.35	0.28 ± 0.04	6.48E−05
AP threshold (mV)	−28.3 ± 5.2	−28.3 ± 3.9	−37.9 ± 5.8	−32.4 ± 4.8	−35.3 ± 4.5	4.41E−08	−32.3 ± 6.0	−34.5 ± 9.1	0.400
AP amplitude (mV)	75.9 ± 11.5	70.9 ± 12.6	94.1 ± 4.5	79.8 ± 14.6	86.3 ± 10.6	5.58E−06	81.5 ± 12.9	69.4 ± 20.8	0.036
Firing frequency per 100 pA	17.6 ± 5.1	22.7 ± 3.9	10.6 ± 3.5	21.4 ± 8.2	13.3 ± 6.2	1.01E−06	16.2 ± 6.7	52.1 ± 20.7	3.38E−17
ISI (ms)	58.1 ± 12.5	75.3 ± 44.8	73.8 ± 29.9	81.8 ± 27.8	107.4 ± 74.0	7.80E−03	81.9 ± 52.5	16.2 ± 12.2	3.06E−03
Min. ISI (ms)	14.0 ± 7.8	11.2 ± 12.6	17.3 ± 8.2	22.4 ± 10.9	26.0 ± 12.2	1.07E−04	19.2 ± 11.8	6.2 ± 2.0	8.49E−03
Max. frequency (Hz)	100.3 ± 58.0	155.2 ± 76.4	78.7 ± 47.6	61.5 ± 43.7	51.6 ± 35.3	3.58E−06	82.8 ± 59.8	166.8 ± 38.3	1.06E−03
Adaptation ratio	0.67 ± 0.11	0.55 ± 0.30	0.56 ± 0.25	0.51 ± 0.22	0.50 ± 0.21	0.044	0.57 ± 0.21	0.85 ± 0.14	1.64E−03
AHP amplitude (mV)	11.8 ± 3.2	12.2 ± 3.2	10.0 ± 2.4	11.5 ± 2.1	10.9 ± 2.2	0.299	11.3 ± 2.7	21.0 ± 6.1	1.40E−11

been observed for the axonal domain of L6B iPCs. Furthermore, the axons of both L6B pyramidal cell subtypes can be traced in the white matter where they project in the direction of the striatum and/or the thalamus, suggesting a corticothalamic or corticostriatal innervation (Fig. 7*A2, B2*).

Discussion

We characterized neurons in sublamina B of neocortical layer 6 on the basis of their functional and structural properties by using single cell recordings in acute brain slices of the primary somatosensory barrel cortex. Our experiments were performed using P17–24 adolescent rats so that L6B neurons (which are the earliest generated neocortical neurons) are likely to have an almost adult morphology (Ferrer and Martinez-Matos 1981; Valverde et al. 1989). To exclude a possible bias in assigning neurons to different groups, we used an unsupervised CA based on the electrophysiological characteristics, direct measurements of axonal, and dendritic parameters (such as length and branching frequency) as well as the relationship between the dendritic and axonal projection pattern and the barrel column. Therefore, our study provides a detailed classification of excitatory L6B neurons based on a quantitative analysis of their functional and structural parameters. We identified a highly heterogeneous neuronal cell population in layer 6B and identified three distinct main clusters of excitatory L6B cell types. These were categorized as (C1) L6B neurons with a main apical dendrite oriented towards the pial surface, that is L6B pyramidal cells, (C2) L6B neurons with a dominant "apical"-like dendrite not oriented towards the pial surface, and (C3) L6B multipolar neurons without any preferential direction. A further subclassification led to the identification of three subgroups within the second cluster based on the orientation of the "apical"-like main dendrite. We named these subgroups inverted neurons (C2a), "tangentially" oriented neurons (C2b), and "horizontally" oriented neurons (C2c).

Previous Studies

Layer 6 occupies about one-third of the neocortex and is clearly subdivided into two separate laminae, layers 6A and 6B. Lamina 6A occupies more than two-thirds of layer 6 while L6B occupies less than one-third (Peters and Jones 1984; Tömböl 1984; Ferrer et al. 1986a, 1986b; Valverde et al. 1989; Zhang and Deschenes 1997; Meyer et al. 2010; Oberlaender et al. 2011; Perrenoud et al. 2012). Furthermore, several studies have described a possible correlation to subplate (SP) neurons. This heterogeneous neuronal cell population perists at least in part in layer 6B into adulthood (Kostovic and Rakic 1980; Reep and Goodwin 1988; Woo et al. 1991). It has been suggested that 10–20% or more SP neurons survive as L6B neurons (Torres-Reveron and Friedlander 2007; Friedlander and Torres-Reveron 2009). Our data suggest that L6B neurons are comparable with different cell types of the SP, especially to "horizontally" oriented, inverted, and multipolar or tripolar SP neurons described earlier (Hanganu et al. 2002; Luhmann et al. 2009; Kanold and Luhmann 2010).

Only few studies of excitatory L6 neurons attempted a quantitative classification using an unsupervised CA. However, they differ markedly in their experimental approach and none concentrated exclusively on neurons in sublamina 6B. An in-vitro study by Andjelic et al. (2009) identifies nonpyramidal neurons in layer 6 (in addition to excitatory neurons from other cortical layers) but does not distinguish between different sublaminae or provide a description of their axonal projection pattern. Moreover, they investigated the expression of molecular markers in combination with electrophysiological properties. This approach led to three clusters, two of which contain L6 neurons, although the CA did not separate different neuronal cell types according to their laminar position. Using Golgi stains, Chen et al. (2009) analyzed neurons in the entire lamina 6 of the barrel cortex using several somatodendritic parameters. Here, the CA resulted in six clusters including two nonpyramidal cell groups, one interneuron group, and three pyramidal cell groups, one of which includes both neurons with short and atypically oriented dendrites. The limited number of parameters and the fact that AP firing properties and the axonal morphology were not investigated as well as the detailed subgrouping makes a comparison with our study difficult. A recent in-vivo labeling study (Pichon et al. 2012) describes very extensive axonal projections of L6 pyramidal neurons, in particular at the level of layer 4. The authors used a CA largely based on axonal parameters such as the bouton density and the axon columnarity. However, the laminar position of most of these neurons was in the upper third of layer 6. It is therefore highly likely that these neurons are L6A pyramidal cells; no nonpyramidal neurons were analyzed in this study.

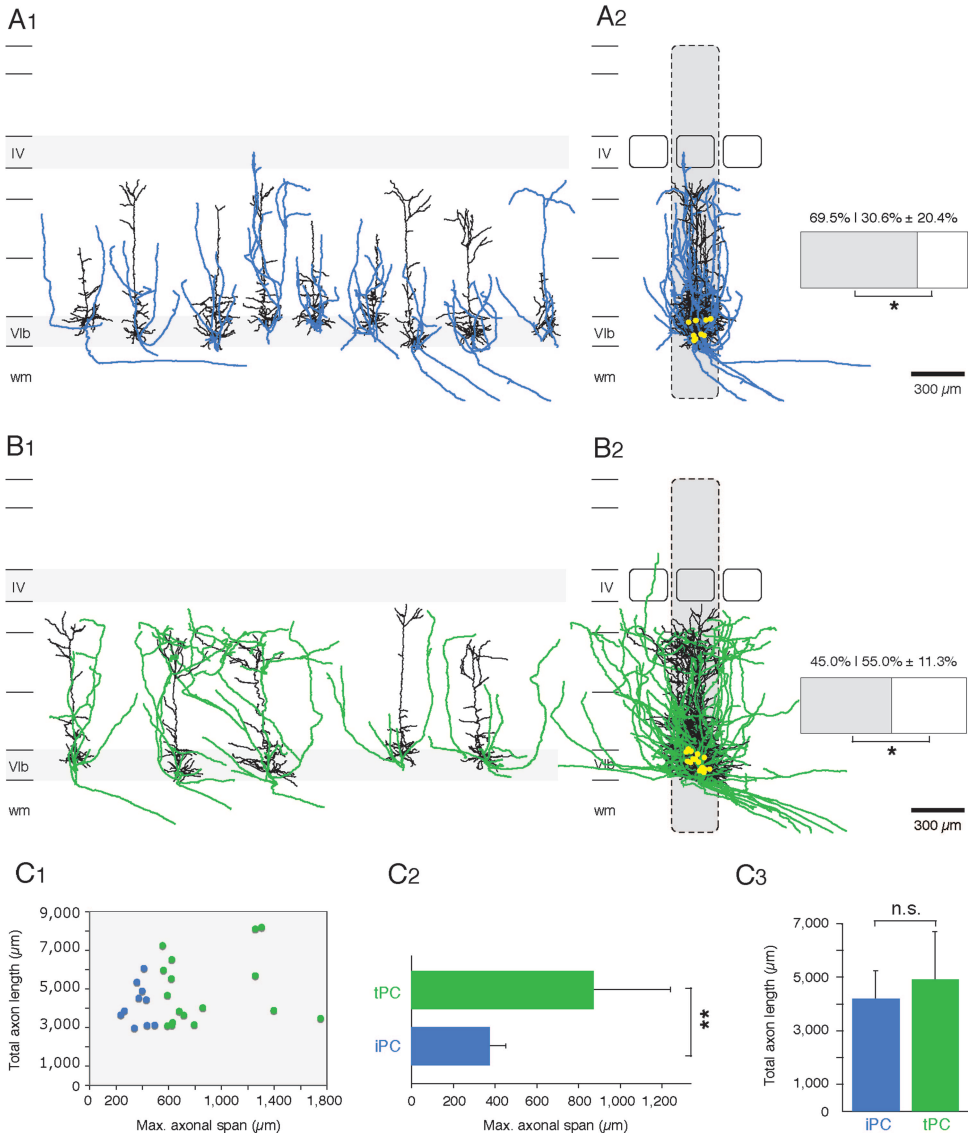

Figure 7. Subtypes of L6B pyramidal cells. Two L6B pyramidal cell subtypes could be identified based on an additional analysis of their axonal domain. L6B pyramidal neurons were designated as iPC and tPC, respectively. (*A1*) Nine example reconstructions of iPCs are shown with their relative position in a cortical column of the somatosensory barrel cortex. (*A2*) Overlay of all 10 iPCs. The reconstructions are superimposed and aligned to the barrel center. Barrels are presented by rectangles and the home barrel column in gray, respectively. IPCs have an axonal columnarity of 69.5 ± 20.4%; that of tPCs is about 45.0 ± 11.3% with a significant difference between both pyramidal subtypes of $P < 0.00048$. (*B1*, *B2*) the same as in *A1* and *A2* only for five example reconstructions and for an overlay of all 17 tPCs. (*C1*) Scatter plot that shows no clear correlation between the total axon length and the maximal axonal field span. We have found pyramidal neurons with a high axon length and a broad axonal field span as well as neurons with a high axon length and a small axonal field span, respectively. (*C2*) Bar diagram of the maximal axonal field span. TPCs have a significant higher axonal field span than iPCs. (*C3*) Total axon length of iPCs and tPCs without any significant difference. Axonal data of iPCs are represented in light blue and that of tPCs in green, respectively. The hippocampus is located on the left and the striatum on the right. Scale bars in *A1,2*, *B1,2*: 300 µm. *, $P < 0.01$, **, $P < 0.001$, n.s. (not significant; $P > 0.1$).

L6B Nonpyramidal Cells

Most spiny, presumably excitatory L6B neurons belong to the group of atypically oriented pyramidal-like neurons and nonpyramidal neurons (~70%; Tömböl et al. 1975; Feldman and Peters 1978; Tömböl 1984; Ferrer et al. 1986a, 1986b; Valverde et al. 1989; Bourassa and Deschenes 1995; Bourassa et al. 1995; Andjelic et al. 2009; Chen et al. 2009). All of our excitatory L6B nonpyramidal neurons have a high density of dendritic spines, a morphological criterion typical for excitatory neurons in the cortex (see e.g. Larkman 1991). Our CA revealed two clearly distinct groups: neurons with a main dendrite projecting in various directions (i.e. atypically oriented pyramidal-like neurons) and multipolar neurons. The occurrence of atypically oriented pyramidal-like neurons, that is inverted (11.5%), "tangential" (11.5%), and "horizontal" (10.3%) neurons is in accordance with previous findings based solely on the dendritic morphology (Van der Loos 1965; Lübke and Albus 1989). Axon collaterals of nonpyramidal L6B neurons are not exclusively confined to layer 6 (with the possible exception of the subgroup of inverted L6B neurons), but innervate also upper layer 5, layer 4, and even layers 2/3. In addition, the axons of excitatory nonpyramidal L6B neurons were not confined to their home barrel column but projected often over several adjacent columns. It is not

entirely clear whether these neurons are innervated by thalamic afferents. Layer 6B is the only neocortical layer that shows only minimal if any innervation by VPM or POm or both (Meyer et al. 2010; Wimmer et al. 2010). Inverted neurons show an axonal projection to local layer 6 and some axonal branches towards the secondary somatosensory (S2) and motor cortex. "Tangential" neurons have a very dense and local axon domain, but also project to superficial layers 2/3 as well to the somatosensory cortex (Valverde et al. 1989; Zhang and Deschenes 1997). The axonal domain of "horizontal" neurons with their long, vertically extending axon collaterals suggests that this L6B neuronal cell type might be a source of corticocortical connections in local layer 6 and adjacent barrel columns (Feldman and Peters 1978; Tömböl 1984; Valverde et al. 1989; Zhang and Deschenes 1997); the same applies for "tangential" neurons. They can be interpreted as possible ipsilateral association neurons within an intracortical subsystem.

L6B Pyramidal Cells

A fraction of about 30% of all L6B neurons are pyramidal cells. These L6B pyramidal neurons showed morphological similarities with those in neocortical lamina 6A. L6A pyramidal neurons reside in the upper two-thirds of layer 6; previous studies (Zhang and Deschenes 1997; Kumar and Ohana 2008; Pichon et al. 2012; for reviews see Briggs 2010; Thomson 2010) have broadly classified them into corticothalamically (CT) and corticocortically (CC) projecting neurons on the basis of their axonal projection pattern. L6A CT pyramidal cells have an axonal domain that is largely confined to the home barrel column. In contrast, L6A CC axons project into the adjacent barrel columns. We hypothesize that the L6B iPC are similar to the L6A CT pyramidal neurons and may project back at least to the striatum. However, we cannot identify the existence of projections to the thalamus, that is to the VPm or POm nucleus as it is the case for L6A CT pyramidal cells (Bourassa et al. 1995). Even if this were the case, L6B iPC neurons cannot be elements of a direct thalamo-cortico-thalamic feedback loop (like L6A CT neurons) because of the lack of thalamic innervation in L6B (Meyer et al. 2010; Wimmer et al. 2010).

The axonal morphology of L6B tPC neurons resmbles that of L6A CC pyramidal neurons: Thus, these neurons may serve to innervate other cortical areas such as the S2 or motor cortex (Zhang and Deschenes 1997; Kumar and Ohana 2008; Pichon et al. 2012). Further, the occurrence of iPCs in layer 6B is with 27% substantially lower than that of tPCs (about 63%). Compared with previous studies L6A CT pyramids account for about 50% in the rat somatosensory and cat visual cortex (Gilbert and Kelly 1975; Zhang and Deschenes 1997; Pichon et al. 2012). This could indicate that L6B pyramidal neurons are more involved in corticocortical signaling than L6A pyramidal cells. In agreement with Pichon and coworkers (Pichon et al. 2012), we hypothesize that the orientation of the main axon can predict the axonal projection pattern to other cortical and subcortical areas. According to this assumption, the direction of L6B axon collaterals in the white matter is indicative for a corticostriatal or corticothalamic projection while that of intracortical long-range collaterals suggests an innervation of the S2 cortex, long-range projections in the white matter may target the striatum, the thalamus, and at least for the tPCs to some extent also the corpus callosum. The dendritic and axonal domains of CT and CC L6A pyramidal cells (Zhang and Deschenes 1997; Kumar and Ohana 2008; Pichon et al. 2012) correlate very well with those of L6B iPCs and tPCs, respectively. However, while L6A pyramidal cells, in particular those in the more superficial part, receive inputs from both the VPM and POm thalamic nuclei, this is not the case for L6B pyramidal neurons.

L6B Interneurons

Interneurons of all neocortical layers including layer 6 have been found to be highly diverse (Ascoli et al. 2008). A recent quantitative study (Perrenoud et al. 2012) used the expression of certain molecular markers, active and passive electrophysiological characteristics, and a few basic morphological properties. Four distinct interneuron clusters in cortical laminae 6A and 6B were identified, namely either late or stuttering fast-spiking parvalbumin-expressing (FS-PV), adapting somatostatin-expressing (SOM), adapting neuropeptide Y-expressing (NPY), and adapting vasoactive intestinal peptide-expressing (VIP) interneurons. We have found interneurons with a stuttering FS pattern and those with an adapting firing pattern which are comparable with FS-PV and adapting SOM or adapting VIP interneuron groups, respectively. We have further identified a few continuously firing FS interneurons that have not been identified in the study by Perrenoud et al. (2012). However, interneurons were not the focus of our study and just served as an internal control group for the CA. In this CA, L6B interneurons constituted as an entirely separate group, thus validating our approach.

Possible Functional Role of Excitatory L6B Neurons

It is not straightforward to assign a functional role to L6B neurons because their axonal projection pattern differs significantly from one another. Excitatory L6B nonpyramidal neurons predominantly establish corticocortical connections (Arimatsu et al. 2003). Further, Arimatsu et al. (2003) found a coexpression of the nuclear receptor-related 1 protein (Nurr1) and latexin, a carboxypeptidase A inhibitor in neurons located also in sublamina 6B. Neurons that are Nurr1 positive contribute predominantly to long-range ipsilateral corticocortical projections (Andjelic et al. 2009). It is likely that a substantial fraction of neurons in this layer is still functionally active in adulthood. However, nonpyramidal neurons in layer 6 (6B) send little or no projections to the thalamus (Prieto and Winer 1999) and do not contribute to callosal projections. They are mostly involved in local and long-distance intrahemispheric circuitry (Divac et al. 1987; Vandevelde et al. 1996; Zhang and Deschenes 1997; Clancy and Cauller 1999). In addition, a previous study demonstrated that L6B neurons in contrast to L6A neurons are highly sensitive for hypocretin-orexin (Bayer et al. 2004). Thus, L6B neurons might play a role in modulating wakefulness and stimulate widespread cortical activation. For the frontal premotor cortex axonal projections from layer 6B to layer 1 have been described (Mitchell and Cauller 2001; in this study sublamina 6B is named layer 7). However, in our study none of the L6B neurons had axonal collaterals that extend beyond layers 2/3.

Here we could demonstrate that excitatory L6B neurons are an integral part of an extensive neuronal network in the infragranular layers 5A, 5B, 6A, and 6B (with the exception of inverted neurons whose axonal domain is largely confined to

layer 6). The density of axon collaterals of L6B neurons is high in layers 6A and 6B suggesting strong local neuronal networks. However, some excitatory L6B neurons project even to layers 4 and 2/3. The density of this projection may be significantly larger than observed here because of the high possibility of axon truncation in the slice preparations. Thus, L6B neurons are synaptically connected to virtually all cortical layers, albeit to a different degree. How L6B neurons interact with neurons in other cortical layers remains to be determined.

A large fraction of deep layer 6 neurons (presumably excitatory L6B neurons) have been shown to exhibit corticothalamic projections to both the VPM and POm thalamic nuclei; a minor fraction projects to POm only (Bourassa and Deschenes 1995; Bourassa et al. 1995). In analogy with the corticothalamic projection neurons in layer 6A (Kumar and Ohana 2008), the iPC type of L6B pyramidal cells (with a largely barrel-confined axonal projection pattern) may be a corticothalamic projection neuron. We suggest that these neurons have a modulatory role in thalamic signal transfer although they receive little if any thalamocortical input (in contrast to L6A pyramidal neurons; e.g. Meyer et al. 2010; Wimmer et al. 2010). Future studies are needed to establish the functional roles of the excitatory L6B neurons identified here.

Funding

This work was partially supported by the Helmholtz Foundation and the DFG Research group BaCoFun. Funding to pay the Open Access publication charges for this article was provided by the Central Library of the Research Center Jülich.

Notes

We thank Werner Hucko for his assistance and Dr Karlijn van Aerde for the custom-written macros for Igor software. *Conflict of Interest*: None declared.

References

Agmon A, Connors BW. 1991. Thalamocortical responses of mouse somatosensory (barrel) cortex in vitro. J Neurosci. 41:365–379.

Allendoerfer KL, Shatz CJ. 1994. The subplate, a transient neocortical structure: its role in the development of connections between thalamus and cortex. Annu Rev Neurosci. 17:185–218.

Andjelic S, Gallopin T, Cauli B, Hill EL, Roux L, Badr S, Hu E, Tamas G, Lambolez B. 2009. Glutamatergic nonpyramidal neurons from neocortical layer VI and their comparison with pyramidal and spiny stellate neurons. J Neurophysiol. 101:641–654.

Arimatsu Y, Ishida M, Kaneko T, Ichinose S, Omori A. 2003. Organization and development of corticocortical associative neurons expressing the orphan nuclear receptor Nurr1. J Comp Neurol. 466:180–196.

Ascoli GA, Alonso-Nanclares L, Anderson SA, Barrionuevo G, Benavides-Piccione R, Burkhalter A, Buzsaki G, Cauli B, Defelipe J, Fairen A *et al.* 2008. Petilla terminology: nomenclature of features of GABAergic interneurons of the cerebral cortex. Nature Rev Neurosci. 9:557–568.

Bayer L, Serafin M, Eggermann E, Saint-Mleux B, Machard D, Jones BE, Muhlethaler M. 2004. Exclusive postsynaptic action of hypocretin-orexin on sublayer 6b cortical neurons. J Neurosci. 24:6760–6764.

Bayer SA, Altman J. 1990. Development of layer I and the subplate in the rat neocortex. Exp Neurol. 107:48–62.

Bourassa J, Deschenes M. 1995. Corticothalamic projections from the primary visual cortex in rats: a single fiber study using biocytin as an anterograde tracer. Neuroscience. 66:253–263.

Bourassa J, Pinault D, Deschenes M. 1995. Corticothalamic projections from the cortical barrel field to the somatosensory thalamus in rats: a single-fibre study using biocytin as an anterograde tracer. Eur J Neurosci. 7:19–30.

Briggs F. 2010. Organizing principles of cortical layer 6. Front. Neural Circuits. 4:3.

Cauli B, Porter JT, Tsuzuki K, Lambolez B, Rossier J, Quenet B, Audinat E. 2000. Classification of fusiform neocortical interneurons based on unsupervised clustering. Proc Natl Acad Sci USA. 97:6144–6149.

Chen CC, Abrams S, Pinhas A, Brumberg JC. 2009. Morphological heterogeneity of layer VI neurons in mouse barrel cortex. J Comp Neurol. 512:726–746.

Chun JJ, Shatz CJ. 1989. Interstitial cells of the adult neocortical white matter are the remnant of the early generated subplate neuron population. J Comp Neurol. 282:555–569.

Clancy B, Cauller LJ. 1999. Widespread projections from subgriseal neurons (layer VII) to layer I in adult rat cortex. J Comp Neurol. 407:275–286.

Connors BW, Gutnick MJ. 1990. Intrinsic firing patterns of diverse neocortical neurons. Trends Neurosci. 13:99–104.

DeDiego I, Smith-Fernández A, Fairén A. 1994. Cortical cells that migrate beyond area boundaries: characterization of an early neuronal population in the lower intermediate zone of prenatal rats. Eur J Neurosci. 6:983–997.

Divac I, Marinkovic S, Mogensen J, Schwerdtfeger W, Regidor J. 1987. Vertical ascending connections in the isocortex. Anat Embryol (Berl). 175:443–455.

Dodt HU, Zieglgansberger W. 1990. Visualizing unstained neurons in living brain slices by infrared DIC-videomicroscopy. Brain Res. 537:333–336.

Feldman ML, Peters A. 1978. The forms of non-pyramidal neurons in the visual cortex of the rat. J Comp Neurol. 179:761–793.

Feldmeyer D, Egger V, Lübke J, Sakmann B. 1999. Reliable synaptic connections between pairs of excitatory layer 4 neurones within a single "barrel" of developing rat somatosensory cortex. J Physiol. 521(Pt 1):169–190.

Feldmeyer D, Lübke J, Sakmann B. 2006. Efficacy and connectivity of intracolumnar pairs of layer 2/3 pyramidal cells in the barrel cortex of juvenile rats. J Physiol. 575:583–602.

Ferrer I, Fabregues I, Condom E. 1986a. A Golgi study of the sixth layer of the cerebral cortex. I. The lissencephalic brain of Rodentia, Lagomorpha, Insectivora and Chiroptera. J Anat. 145:217–234.

Ferrer I, Fabregues I, Condom E. 1986b. A Golgi study of the sixth layer of the cerebral cortex. II. The gyrencephalic brain of Carnivora, Artiodactyla and Primates. J Anat. 146:87–104.

Ferrer I, Martinez-Matos JA. 1981. Development of non-pyramidal neurons in the rat somatosensory cortex during the fetal and early postnatal periods. J Hirnforsch. 22:555–562.

Friedlander MJ, Torres-Reveron J. 2009. The changing roles of neurons in the cortical subplate. Front Neuroanat. 3:15.

Garweg G. 1970. Differential incorporation into cell layers of the cerebral cortex following labelling with D,L-proline-H3 in mice. Experientia. 26:1348–1349.

Gilbert CD, Kelly JP. 1975. The projection of cells in different layers of the cat's visual cortex. J Comp Neurol. 163:81–106.

Glaser JR, Glaser EM. 1990. Neuron imaging with Neurolucida—a PC-based system for image combining microscopy. Comput Med Imaging Graph. 14:307–317.

Hanganu IL, Kilb W, Luhmann HJ. 2002. Functional synaptic projections onto subplate neurons in neonatal rat somatosensory cortex. J Neurosci. 22:7165–7176.

Helmstaedter M, Feldmeyer D. 2010. Axons predict neuronal connectivity within and between cortical columns and serve as primary classifiers of interneurons in a cortical column. In: Feldmeyer D, Lübke J, editors. New aspects of axonal structure and function. New York, Dordrecht, Heidelberg, London: Springer Science + Business Media.

Helmstaedter M, Sakmann B, Feldmeyer D. 2009a. Neuronal correlates of local, lateral, and translaminar inhibition with reference to cortical columns. Cereb Cortex. 19:926–937.
Helmstaedter M, Sakmann B, Feldmeyer D. 2009b. The relation between dendritic geometry, electrical excitability, and axonal projections of L2/3 interneurons in rat barrel cortex. Cereb Cortex. 19:938–950.
Helmstaedter M, Sakmann B, Feldmeyer D. 2009c. L2/3 interneuron groups defined by multiparameter analysis of axonal projection, dendritic geometry, and electrical excitability. Cereb Cortex. 19:951–962.
Hogan D, Berman NE. 1992. The development of neuropeptide Y immunoreactive neurons in cat visual cortical areas. Brain Res Dev Brain Res. 67:343–369.
Kanold PO, Luhmann HJ. 2010. The subplate and early cortical circuits. Annu Rev Neurosci. 33:23–48.
Kawaguchi Y, Kubota Y. 1993. Correlation of physiological subgroupings of nonpyramidal cells with parvalbumin- and calbindinD28k-immunoreactive neurons in layer V of rat frontal cortex. J Neurophysiol. 70:387–396.
Kawaguchi Y, Kubota Y. 1997. GABAergic cell subtypes and their synaptic connections in rat frontal cortex. Cereb Cortex. 7: 476–486.
Kirsche W, Kunz G, Wenzel J, Winkelmann E, Wenzel M, Winkelmann A. 1973. Neurohistological studies on the variability of the pyramidal cells of the sensory cortex of the rat. J Hirnforsch. 14:117–135.
König N, Roch G, Marty R. 1975. The onset of synaptogenesis in rat temporal cortex. Anat Embryol (Berl). 148:73–87.
König N, Valat J, Fulcrand J, Marty R. 1977. The time of origin of Cajal-Retzius cells in the rat temporal cortex. An autoradiographic study. Neurosci Lett. 4:21–26.
Kostovic I, Rakic P. 1980. Cytology and time of origin of interstitial neurons in the white matter in infant and adult human and monkey telencephalon. J Neurocytol. 9:219–242.
Kristt DA. 1979b. Development of neocortical circuitry: histochemical localization of acetylcholinesterase in relation to the cell layers of rat somatosensory cortex. J Comp Neurol. 186:1–15.
Kumar P, Ohana O. 2008. Inter- and intralaminar subcircuits of excitatory and inhibitory neurons in layer 6a of the rat barrel cortex. J Neurophysiol. 100:1909–1922.
Land PW, Kandler K. 2002. Somatotopic organization of rat thalamocortical slices. J Neurosci Methods. 119:15–21.
Larkman AU. 1991. Dendritic morphology of pyramidal neurones of the visual cortex of the rat: III. Spine distributions. J Comp Neurol. 306:332–343.
Lübke J, Albus K. 1989. The postnatal development of layer VI pyramidal neurons in the cat's striate cortex as visualized by intracellular Lucifer yellow injections in aldehyde-fixed tissue. Dev Brain Res. 45:29–38.
Lübke J, Markram H, Frotscher M, Sakmann B. 1996. Frequency and dendritic distribution of autapses established by layer 5 pyramidal neurons in the developing rat neocortex: comparison with synaptic innervation of adjacent neurons of the same class. J Neurosci. 16:3209–3218.
Lübke J, Roth A, Feldmeyer D, Sakmann B. 2003. Morphometric analysis of the columnar innervation domain of neurons connecting layer 4 and layer 2/3 of juvenile rat barrel cortex. Cereb Cortex. 13:1051–1063.
Luhmann HJ, Kilb W, Hanganu-Opatz IL. 2009. Subplate cells: amplifiers of neuronal activity in the developing cerebral cortex. Front Neuroanat. 3:19.
Luskin MB, Shatz CJ. 1985. Neurogenesis of the cat's primary visual cortex. J Comp Neurol. 242:611–631.
Marín-Padilla M. 1978. Dual origin of the mammalian neocortex and evolution of the cortical plate. Anat Embryol (Berl). 152:109–126.
Marx M, Günter RH, Hucko W, Radnikow G, Feldmeyer D. 2012. Improved biocytin labeling and neuronal 3D reconstruction. Nat Protoc. 7:394–407.
McCormick DA, Connors BW, Lighthall JW, Prince DA. 1985. Comparative electrophysiology of pyramidal and sparsely spiny stellate neurons of the neocortex. J Neurophysiol. 54:782–806.
McDonald CT, Burkhalter A. 1993. Organization of long-range inhibitory connections with rat visual cortex. J Neurosci. 13: 768–781.
Meyer HS, Wimmer VC, Oberlaender M, de Kock CP, Sakmann B, Helmstaedter M. 2010. Number and laminar distribution of neurons in a thalamocortical projection column of rat vibrissal cortex. Cereb Cortex. 20:2277–2286.
Miller MW, Potempa G. 1990. Numbers of neurons and glia in mature rat somatosensory cortex: effects of prenatal exposure to ethanol. J Comp Neurol. 293:92–102.
Mitchell BD, Cauller LJ. 2001. Corticocortical and thalamocortical projections to layer I of the frontal neocortex in rats. Brain Res. 921:68–77.
Oberlaender M, de Kock CP, Bruno RM, Ramirez A, Meyer HS, Dercksen VJ, Helmstaedter M, Sakmann B. 2011. Cell type-specific three-dimensional structure of thalamocortical circuits in a column of rat vibrissal cortex. Cereb Cortex. 1–17.
Ohana O, Sakmann B. 1998. Transmitter release modulation in nerve terminals of rat neocortical pyramidal cells by intracellular calcium buffers. J Physiol. 513:135–148.
Perrenoud Q, Rossier J, Geoffroy H, Vitalis T, Gallopin T. 2012. Diversity of GABAergic interneurons in layer VIa and VIb of mouse barrel cortex. Cereb Cortex. doi: 10.1093/cercor/bhs032.
Peters A, Jones EG. 1984. Cellular components in the cerebral cortex. In: Peters A, Jones EG, editors. Cerebral Cortex. London (NY): Plenum Press. 1:107–121
Pichon F, Nikonenko I, Kraftsik R, Welker E. 2012. Intracortical connectivity of layer VI pyramidal neurons in the somatosensory cortex of normal and barrelless mice. Eur J Neurosci. 35:855–869.
Prieto JJ, Winer JA. 1999. Layer VI in cat primary auditory cortex: Golgi study and sublaminar origins of projection neurons. J Comp Neurol. 404:332–358.
Radnikow G, Günter GH, Marx M, Feldmeyer D. 2012. Morphofunctional mapping of cortical networks in brain slice preparations using paired electrophysiological recordings. In: Fellin T, Halassas M, editors. Neuronal network analysis. New York (NY): Humana Press: An Imprint of Springer Science+Business Media.
Reep RL, Goodwin GS. 1988. Layer VII of rodent cerebral cortex. Neurosci Lett. 90:15–20.
Rose M. 1931. Cytoarchitektonischer Atlas der Grosshirnrinde des Kaninchens. J Psychol Neurol. 43:353–440.
Stuart GJ, Dodt HU, Sakmann B. 1993. Patch-clamp recordings from the soma and dendrites of neurons in brain slices using infrared video microscopy. Pflugers Arch. 423:511–518.
Thomson AM. 2010. Neocortical layer 6, a review. Front Neuroanat. 4:13.
Thomson AM, West DC, Hahn J, Deuchars J. 1996. Single axon IPSPs elicited in pyramidal cells by three classes of interneurones in slices of rat neocortex. J Physiol. 496(Pt 1):81–102.
Thorndike RL. 1953. Who belongs in the family. Psychometrika. 18:267–276.
Tömböl T. 1984. Layer VI cells. In: Peters A, Jones EG, editors. Cerebral Cortex. London (NY): Plenum Press. 1:479–510
Tömböl T, Hajdu F, Somogyi G. 1975. Identification of the Golgi picture of the layer VI cortic-geniculate projection neurons. Exp Brain Res. 24:107–110.
Torres-Reveron J, Friedlander MJ. 2007. Properties of persistent postnatal cortical subplate neurons. J Neurosci. 27:9962–9974.
Valverde F, Facal-Valverde MV, Santacana M, Heredia M. 1989. Development and differentiation of early generated cells of sublayer VIb in the somatosensory cortex of the rat: a correlated Golgi and autoradiographic study. J Comp Neurol. 290:118–140.
van der Loos H. 1965. The "improperly" oriented pyramidal cell in the cerebral cortex and its possible bearing on problems of neuronal growth and cell orientation. Bull Johns Hopkins Hosp. 117:228–250.

Vandevelde IL, Duckworth E, Reep RL. 1996. Layer VII and the gray matter trajectories of corticocortical axons in rats. Anat Embryol (Berl). 194:581–593.
Vogt C, Vogt O. 1919. Allgemeinere Ergebnisse unserer Hirnforschung. J Psychol Neurol. 25:292–398.
von Economo C, Koskinas GN. 1925. Die Cytoarchitektonik der Hirnrinde des erwachsenen Menschen. Wien: Springer Verlag.
Ward JH, Jr. 1963. Hierarchical grouping to optimize an objective function. Am Stat Assoc. 58:236–244.
Wimmer VC, Bruno RM, de Kock CP, Kuner T, Sakmann B. 2010. Dimensions of a projection column and architecture of VPM and POm axons in rat vibrissal cortex. Cereb Cortex. 20: 2265–2276.
Woo TU, Beale JM, Finlay BL. 1991. Dual fate of subplate neurons in a rodent. Cereb Cortex. 1:433–443.
Zhang ZW, Deschenes M. 1997. Intracortical axonal projections of lamina VI cells of the primary somatosensory cortex in the rat: a single-cell labeling study. J Neurosci. 17:6365–6379.